

Rapid Solid-State Synthesis of Refractory Nitrides

Edward G. Gillan and Richard B. Kaner*

Department of Chemistry and Biochemistry and Solid State Science Center, University of California, Los Angeles, California 90024-1569

Received March 7, 1994[⊗]

Rapid solid-state metathesis (SSM) reactions are used to synthesize a series of refractory transition-metal nitrides. Exothermic reactions of metal halides with Li_3N and/or NaN_3 produce the mononitrides (TiN , ZrN , HfN , NbN , and TaN) as crystalline powders. The partial substitution of sodium azide for lithium nitride favors the formation of nitrogen-rich phases. In some cases, achieving a high reaction temperature and large internally generated nitrogen gas pressure enables the formation of nitride phases normally only synthesized at high temperatures and pressures (e.g. cubic NbN and TaN). Powder X-ray diffraction, magnetic susceptibility, electron microscopy, thermal and elemental analysis are used to characterize the compounds. All of the mononitrides are cubic with an NaCl structure (except TaN which also contains a hexagonal phase) and have lattice parameters that are consistent with nearly stoichiometric products. The superconducting transition temperatures for ZrN (8.5 K) and NbN (15.5 K) are also indicative of metal to nitrogen ratios near unity. These rapid reactions produce crystallites with average sizes near 500 Å (as determined from X-ray line broadening) with size variation possible through changes in the reaction conditions. Differential scanning calorimetry and *in situ* reaction temperature measurements on the ZrN system indicate that initiation occurs when one precursor undergoes a phase change or decomposes. The result is a rapid self-propagating reaction which reaches temperatures of nearly 1370 °C within half of a second of initiation followed by rapid cooling to near room temperature within 30 s. The measured maximum reaction temperature agrees well with a theoretical value (1408 °C) calculated assuming an adiabatic system.

The early transition metals belonging to group four (Ti, Zr, and Hf) and group five (V, Nb, and Ta) all form very stable compounds with nitrogen. The most important of these are the mononitrides ($\text{MN}_{1.0}$) which are quite hard (8–9 on the Mohs scale) and refractory with melting points near 3000 °C.¹ They exhibit metallic conductivity and some show superconductivity (e.g. ZrN : $T_c \approx 10$ K and NbN : $T_c \approx 16$ K).^{2,3} These nitrides are generally resistant to chemical attack and stable at high temperatures in inert or reducing atmospheres.⁴ They have found uses as hard, protective coatings for cutting tools⁵ and UHV system components.⁶ Dense crucibles of ZrN and TiN have served as vessels for the melting of metals.⁴ Recently the superconductivity of NbN has been exploited to make superconducting coatings in radiofrequency cavities⁷ and TiN has shown promise as a diffusion barrier in microelectronics.⁸

Traditionally these nitrides are synthesized by the direct reaction of the metals with nitrogen or ammonia at temperatures near 1200 °C for extended periods of time.^{1,9} Chemical vapor deposition of metal chlorides with NH_3 or N_2/H_2 mixtures at 1000 °C can produce metal nitride thin films.¹⁰ The low-temperature decomposition of organometallic precursors is a recently developed route to nitrogen-rich nitride films.¹¹ Self-propagating high-temperature synthesis (SHS) can also be

utilized to form nitrides by heating or igniting fine metal powders in the presence of high nitrogen pressures or by using sodium azide as a solid source of nitrogen.¹² This combustion process results in nitride powder formation, though these reactions are often incomplete, leaving unreacted metal or lower nitrides in the product.¹³

In recent years there has been increasing interest in nontraditional synthetic routes to solid state compounds sparked by a desire for materials with improved or controllable properties (e.g. crystallite size, composition, microstructure, etc.). Solid-state metathesis (SSM) reactions have been developed as rapid and successful routes to a wide variety of materials.^{14–16} Recent examples include the synthesis of metal chalcogenides and pnictides from high oxidation state metal halides reacted with

[⊗] Abstract published in *Advance ACS Abstracts*, November 1, 1994.

- Toth, L. E. *Refractory Materials, Vol. 7: Transition Metal Carbides and Nitrides*; Academic Press: New York, 1971.
- Storms, E. K. In *MTP Review of Science: Solid State Chemistry*; Roberts, L. E. J., Ed.; University Park Press: Baltimore, Md., 1972; Vol. 10 (Series 1), pp 37–78.
- Lengauer, W. *Surf. Interface Anal.* **1990**, *15*, 377.
- Blocher, J. M., Jr. In *High Temperature Technology*; Campbell, I. E., Ed.; John Wiley and Sons, Inc.: New York, 1956; pp 171–186.
- (a) Buhl, R.; Pulker, H. K.; Moll, E. *Thin Solid Films* **1981**, *80*, 265. (b) Sundgren, J. E. *Thin Solid Films* **1985**, *128*, 21.
- Moriyama, K. *Mat. Res. Soc. Bull.* **1990**, *15*(7), 32.
- (a) Fabbriatore, P.; Fernandes, P.; Gualco, G. C.; Merlo, F.; Musenich, R.; and Parodi, R. *J. Appl. Phys.* **1989**, *66*(12), 5944. (b) Kampwirth, R. T.; Gray, K. E. *IEEE Trans. Mag.* **1981**, *17*(1), 565.
- Östling, M.; Nygren, S.; Petersson, C. S.; Norström, H.; Buchta, R.; Blom, H. O.; Berg, S. *Thin Solid Films* **1986**, *145*, 81.

- (a) Blumenthal, W. B. *Chemical Behavior of Zirconium*; Van Nostrand: Princeton, NJ, 1958; pp 46–92. (b) Fabbriatore, P.; Musenich R.; Ochetto, M.; Parodi, R.; Pompa, P. *IEEE Trans. Mag.* **1991**, *27*(2), 1291. (c) Brauer, G.; Esselborn, R. *Z. Anorg. Allg. Chem.* **1961**, *309*, 151.
- (a) Nakanishi, N.; Mori, S.; Kato, E. *J. Electrochem. Soc.* **1990**, *137*(1), 322. (b) Buiting, M. J.; Otterloo, A. F.; Montree, A. H. *J. Electrochem Soc.* **1991**, *138*(2), 500.
- (a) Fix, R.; Gordon, R. G.; Hoffman, D. M. *Chem. Mater.* **1991**, *3*, 1138. (b) Fix, R.; Gordon, R. G.; Hoffman, D. M. *Chem. Mater.* **1993**, *5*, 614.
- (a) Munir, Z. A. *Ceram. Bull.* **1988**, *67*(2), 342. (b) Yi, H. C.; Moore, J. J. *J. Mat. Sci.* **1990**, *25*, 1159. (c) Holt, J. B. *Ind. Res. Dev.* **1983**, *Apr*, 88. (d) Holt, J. B. U.S. Patent Nos. 4,446,242 (May 1, 1984) and 4,459,363 (July 10, 1984).
- (a) Eslamoo-Grami, M.; Munir, Z. A. *J. Am. Ceram. Soc.* **1990**, *73*(8), 2222. (b) Deevi, S.; Munir, Z. A. *J. Mater. Res.* **1990**, *5*(10), 2177.
- Wiley, J. B.; Kaner, R. B. *Science* **1992**, *255*, 1093.
- (a) Wiley, J. B.; Bonneau, P. R.; Treece, R. E.; Jarvis, R. F.; Gillan, E. G.; Rao, L.; Kaner, R. B. In *Supramolecular Architecture: Synthetic Control in Thin Films and Solids*, Bein, T., Ed.; ACS Symposium Series 499; American Chemical Society: Washington, DC, 1991; Bein, T. Ed.; pp 369–383. (b) Kaner, R. B.; Bonneau, P. R.; Gillan, E. G.; Wiley, J. B.; Treece, R. E. U.S. Patent No. 5,110,768 (May 5, 1992).
- (a) Treece, R. E.; Gillan, E. G.; Jacobinas, R. M.; Wiley, J. B.; Kaner, R. B. In *Better Ceramics Through Chemistry V*; Hampden-Smith, M. J.; Klemperer, W. J.; Brinker, C. J. Eds.; MRS Symposium Proceedings 271; Materials Research Society: Pittsburgh, PA, 1992; pp 169–174.

alkali-metal pnictides or chalcogenides. Previous work using this type of reaction route has resulted in the rapid synthesis of crystalline NiS₂,¹⁷ MoS₂¹⁸ and its anion (e.g. MoS_{2-x}Se_x) and cation (e.g. Mo_xW_{1-x}S₂) solid solutions,¹⁹ GaAs and other III-V (group 13-15) semiconductors,²⁰ in addition to rare-earth (group 3-15) pnictides,²¹ and transition-metal oxides.²² This method takes advantage of the large exothermic heat of formation of alkali-metal halide salts (~100 kcal/mol) and uses this to produce very rapid and vigorous reactions. The precursors are sometimes so reactive that they self-initiate on mixing. Otherwise, a short external initiation (from a heated filament) will usually cause the reaction to self-propagate. These SSM reactions rapidly reach high temperatures (>1000 °C), and cool very quickly. The precursors are generally readily accessible and allow for the possibility of mixed cation and anion solid-solutions. The products of this type of synthesis are polycrystalline, with average crystallite sizes less than 1000 Å for the more refractory compounds. This can be advantageous for ceramic powder processing since small particles often compact and sinter more easily than larger ones. Small crystallites may also exhibit improved physical properties.²³

In 1906, Gunz and co-workers²⁴ observed that late transition-metal (Fe, Co, and Cu) halides and Li₃N react in an "incandescent" manner when heated to 500 °C, but the products, which were thought to be mixtures of metals and metal nitrides, were not fully characterized and this method was not pursued further. Recent work by Parkin and co-workers²⁵ found that when a wide range of metal chlorides are heated with lithium nitride to 500 °C in sealed tubes, similar violent reactions occur, leading to metal nitrides or metals. Here we report the successful synthesis of group four and five mononitrides using rapid, solid-state metathesis (SSM) reactions. This study follows up on our initial reports of successful metal nitride synthesis.^{14,15} The SSM synthetic route has advantages over other synthetic processes since it requires essentially no external heating and makes use of solid nitrogen-containing precursors which eliminates the need to manipulate high pressure gases (N₂ or NH₃). In this study solid early transition-metal halides are reacted with Li₃N and/or NaN₃ as nitrogen sources. In some cases high-temperature/high-pressure phases are observed, consistent with measured reaction temperatures near 1400 °C.

Experimental Section

Caution! Most solid-state metathesis reactions are highly exothermic and in some cases the precursors may spontaneously react when mixed or ground vigorously. Care should be taken to do reactions of this

type on small scales first (less than one gram of reactant mixture) with adequate safety precautions. These reactions may ignite when exposed to small amounts (a drop) of a solvent such as water or methanol. It is also important to calculate the pressure generated by the nitrogen gas byproduct before performing any reaction, since high gas pressures can lead to explosions.

Reagents. The following metal halides were purified prior to use by vapor transport in evacuated (10⁻⁴ Torr) Pyrex tubes across a temperature gradient from the temperatures listed to room temperature: TiI₄ (Alpha, 99%) 120 °C, ZrCl₄ (Aldrich, 99.9%) 350 °C, HfCl₄ (Aesar, 98%) 350 °C, NbCl₅ (Alpha, 99%) 200 °C, and TaCl₅ (Aldrich, 99.9%) 200 °C. TiCl₃ (Johnson-Matthey, 98+%), Li₃N (Cerac, 99.5%), NaN₃ (Sigma, anhydrous), NaCl (Fisher, cert. ACS), Nb (Cerac, 99.8%), and ZrN (Alpha, 99%) were used as received.

Synthesis. Reactions were generally restricted to small scales for safety reasons, since high nitrogen pressures and high temperatures are often generated in these reactions. Typically 2-4 mmol (~1 g) of the metal halide (referred to as small scale reactions) were reacted with a stoichiometric amount of Li₃N and/or NaN₃. In some cases, 20 mmol (~5 g) of the metal halide were used to compare the effect of reaction size (referred to as large scale reactions). The amounts of each reagent used were balanced to leave no excess halogen or alkali metal in the reaction product (referred to as salt-balanced). In each reaction, finely divided reactant powders were ground together with a mortar and pestle in a helium-filled drybox (Vacuum Atmospheres MO-40) and then transferred to a 45 milliliter stainless steel reaction vessel (nonairtight) modeled after a bomb calorimeter.²⁶ The reactions were initiated with a resistively heated nichrome wire (*T* ≈ 850 °C, for ~1 s) placed in the reactant powder mixture. Note that although the reaction vessels are not initially airtight, sometimes the reaction forces the product powders into the seam under the lid which self-seals the container. The products were removed from the drybox, washed with methanol (Fisher, reagent grade) followed by distilled water in order to dissolve away any unreacted starting materials and salt byproducts and then dried in air.

Characterization. Powder X-ray Diffraction. The washed products were examined by powder X-ray diffraction (XRD) using a Crystal Logic θ - 2θ diffractometer equipped with a graphite monochromator and using Cu K α radiation. The scans were taken in the range 10° ≤ 2 θ ≤ 100° at 0.02 or 0.05 degree intervals and three second count times. Lattice parameters and average crystallite sizes were determined relative to crystalline silicon or tungsten internal standards. The crystallite sizes were calculated using the XRD peak broadening and the Scherrer and Warren equations.²⁷ In all cases, the peaks were stripped of their K α ₂ component and fit using a peak analysis program to determine their peak positions and full width at half maximum.²⁸ Lattice parameters were computed using least squares refinement. The XRD results in the figures contain both K α ₁ and K α ₂ components.

Electron Microscopy. Loose powders were attached to graphite disks with colloidal graphite (Ted Pella Co.) and particle morphologies were analyzed by scanning electron microscopy (SEM-Cambridge Stereoscan 250). Energy dispersive spectroscopy (EDS-Tracor Northern TN2000) was performed with 300 s accumulation times to get semi-quantitative elemental analysis on sodium and chlorine in selected samples.

Magnetic Susceptibility. Samples of ZrN and NbN were examined by magnetic susceptibility (SHE Corp. 905 SQUID) to determine their superconducting behavior. Each sample was loaded into an aluminum bucket and field-cooled in a 2 kG field prior to measurement. Sample sizes ranged from 50 to 150 mg and measurements were performed from 5 to 30 K. Data points were taken in 0.5° increments around the transition points.

Elemental Analysis. The metal contents of the large scale, single-phase TiN, ZrN and NbN products were determined from thermogravimetric analysis (TGA-Dupont 951) by converting the nitrides to oxides. Typically 20-30 mg of the nitride was placed in a gold foil cup and

- (17) Bonneau, P. R.; Shibao, R. K.; Kaner, R. B. *Inorg. Chem.* **1990**, *29*, 2511.
 (18) Bonneau, P. R.; Jarvis, Jr., R. F.; Kaner, R. B. *Nature* **1991**, *349*, 510.
 (19) (a) Bonneau, P. R.; Jarvis, Jr., R. F.; Kaner, R. B. *Inorg. Chem.* **1992**, *31*, 2127. (b) Bonneau, P. R.; Kaner, R. B. *Inorg. Chem.* **1993**, *32*, 6084.
 (20) (a) Treece, R. E.; Macala, G. S.; Kaner, R. B. *Chem. Mater.* **1992**, *4*, 9. (b) Treece, R. E.; Macala, G. S.; Rao, L.; Franke, D.; Eckert, H.; Kaner, R. B. *Inorg. Chem.* **1993**, *32*, 2745.
 (21) (a) Fitzmaurice, J. C.; Parkin, I. P.; Rowley, A. T. *J. Mater. Chem.* **1994**, *4*(2), 285. (b) Treece, R. E.; Conklin, J. A.; Kaner, R. B. *Inorg. Chem.*, following paper in this issue.
 (22) (a) Wiley, J. B.; Gillan, E. G.; Kaner, R. B. *Mater. Res. Bull.* **1993**, *28*, 893. (b) Hector, A.; Parkin, I. P. *Polyhedron* **1993**, *12*(15), 1855.
 (23) (a) Ziolo, R. F.; Giannelis, E. P.; Weinstein, B. A.; O'Horo, M. P.; Ganguly, B. N.; Mehrotra, V.; Russell, M. W.; Huffman, D. R. *Science* **1992**, *257*, 219. (b) Fougere, G. E.; Weertman, J. R.; Siegel, R. W.; Kim, S. *Scr. Metall. Mater.* **1992**, *26*, 1879. (c) Siegel, R. W. *Annu. Rev. Mater. Sci.* **1991**, *21*, 559.
 (24) (a) Guntz, A. C. *R. Acad. Sci., Ser. 3* **1902**, *135*, 738. (b) Guntz, A.; Bassett, H. *Bull. Soc. Chim. Paris, Ser. 3* **1906**, *35*, 201.
 (25) (a) Fitzmaurice, J. C.; Hector, A.; Parkin, I. P. *Polyhedron* **1993**, *12*(11), 1295. (b) Fitzmaurice, J. C.; Hector, A. L.; Parkin, I. P. *J. Chem. Soc., Dalton Trans.* **1993**, *16*, 2435.

- (26) Shoemaker, D. P.; Garland, C. W.; Steinfeld, J. I.; Nibler, J. W. *Experiments in Physical Chemistry*, 4th ed.; McGraw-Hill Book Co.: New York, 1981; pp 125-139.
 (27) Warren, B. E. *X-ray Diffraction*; Dover Publications: New York, 1990; pp 251-258.
 (28) XLAB software package by Prof. Dollase, Department of Earth and Space Sciences, University of California, Los Angeles.

heated at 10 °C/min in air to 1000 °C where it remained until its weight was unchanged. The products showed a rapid oxidation when heated to 500 °C in flowing air (30 mL/min). Nitrogen was quantitatively determined using the Kjeldahl technique.²⁹ Samples were dissolved in hot, concentrated H₂SO₄ (300–340 °C) containing 2% K₂SO₄. Solutions with approximately 15 mg of the dissolved nitride were made basic with NaOH and the resulting ammonia was distilled into concentrated boric acid and titrated with standard HCl. These solutions were also analyzed for lithium and sodium (when applicable) contents using ICP-AA spectroscopy (Instruments SA, model JY70PLUS). The combination of these techniques accounted for at least 95% of the product weight. The results found (vs theoretical based on MN_{1.0}) for TiN: Ti, 77.6% (77.4%); N, 18.9% (22.6%); Li, 0.01%; Na, 0.1%; for ZrN: Zr, 84.8% (86.7%); N, 11.1% (13.3%); Li, 0.03%; and for NbN: Nb, 84.6% (86.9%); N, 11.5% (13.1%); Li, 0.05%; Na 0.06%. EDS analysis showed no evidence (<1%) of chlorine in any sample and no sodium in the products when sodium azide was used (TiN and NbN).

Thermal Analysis. Heat of reaction measurements were performed using a standard oxygen bomb calorimeter (Parr, Model 1221). The precursors for ZrN (~2 g) were loaded in the bomb and then ignited in a temperature bath monitored with a digital thermometer. A value for the heat of reaction was obtained from the resulting temperature change and reaction yield. The reaction temperature profile for the ZrN reaction was measured by igniting the precursor mixture (1.5 g) in a modified reaction vessel with 0.1 mm chromel-alumel thermocouple wires inserted into the reactant mixture through a small hole drilled in the bottom of the reactor. The response was recorded on a chart recorder (Linear Instruments Corp., Model 155) with a chart speed of 6.7 mm/sec. The voltage changes were converted to temperatures using the appropriate conversion tables.³⁰ Differential scanning calorimetry (DSC-Dupont 910) was performed on small amounts (~10 mg) of ZrCl₄ with Li₃N or NaN₃, which were lightly pressed into pellets and sealed in aluminum pans. These were monitored in the temperature range of 25–600 °C with a 20 °C/min heating rate under argon in order to observe the reaction initiation and any other thermal events.

Results

Group 4 Nitrides. The reaction of Li₃N with TiCl₃ (or TiCl₄), ZrCl₄, or HfCl₄, produce mononitrides of TiN, ZrN, and HfN, respectively. These products are polycrystalline yellow-brown nitrides which crystallize in the cubic, rock-salt (NaCl) structure. The reaction of the above halides with NaN₃ also produced the cubic mononitrides although elemental sodium appeared in the unwashed products as evidenced by vigorous gas evolution during the methanol wash. The powder XRD result for the small scale reaction forming ZrN is shown in Figure 1a. All major peaks are indexable to a face-centered cubic (*F_m3_m*) structure. The small peak at ~35° corresponds to α-Zr (hcp) although it has a smaller 2θ value than the pure metal. Phase diagrams indicate that this hexagonal metal phase can support a considerable amount of dissolved nitrogen, thus the peak shift indicates that this elemental impurity is partially nitrided, causing the metal lattice to expand.³¹ Large scale reactions forming ZrN produce a cubic, crystalline nitride without zirconium metal (Figure 1b). The chemical yield for the large scale reaction ranged from 80–90%, while the small scale reaction gave a 50–60% yield. Powder XRD shows no metallic impurities although the small peak at ~30° is assigned to the most intense peak (111) of cubic zirconia (ZrO₂). The oxygen likely originates from the lithium nitride precursor since a minor peak in its XRD pattern corresponds to LiOH. Additionally, ZrCl₄ has been shown to form zirconia when it is reacted with alkali

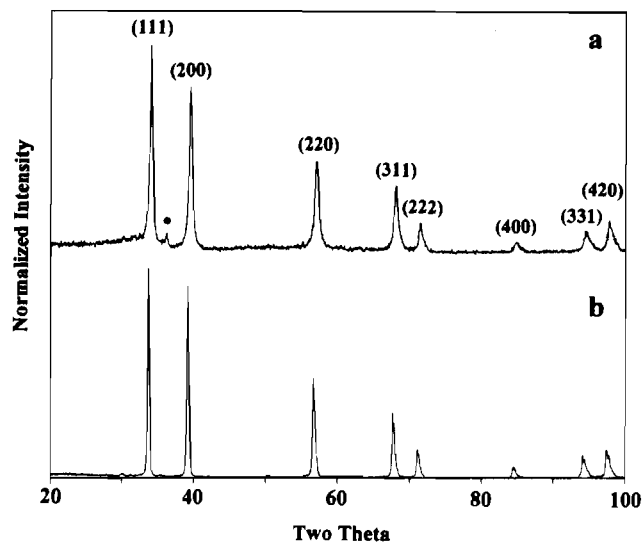


Figure 1. Powder X-ray diffraction patterns of washed products from the rapid SSM reaction between stoichiometric amounts of Li₃N with (a) 4 mmol ZrCl₄ and (b) 20 mmol ZrCl₄. The cubic ZrN peaks are labeled with their (*hkl*) values and the ● denotes α-Zr.

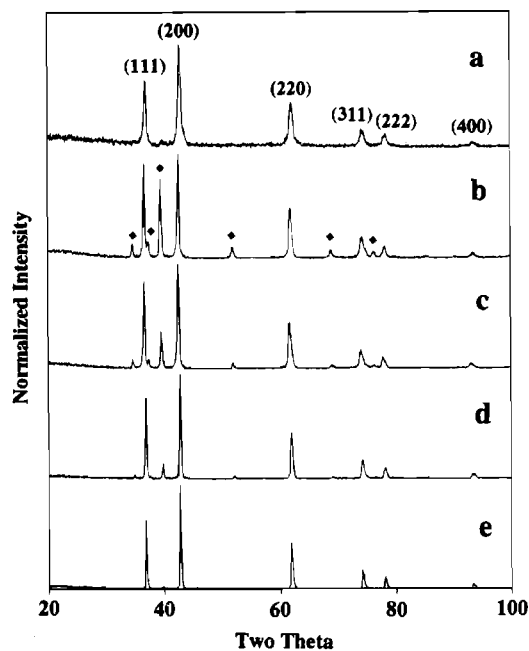


Figure 2. Powder XRD patterns of washed products from reactions forming cubic TiN. Results are from stoichiometric reactions between (a) 4 mmol TiCl₄ and Li₃N; (b) 4 mmol TiCl₃ and Li₃N; (c) 4 mmol TiCl₃ and NaN₃; (d) 20 mmol TiCl₃ and Li₃N; (e) 20 mmol TiCl₃ and Li₃N:NaN₃ (1:1.5). The cubic TiN peaks are labeled with their (*hkl*) values and the ◆ denotes α-Ti.

metal oxides.^{16,22} The XRD pattern of the small scale HfN product is qualitatively similar to that of ZrN.

In the case of TiN, Figures 2a and 2b show that the amount of titanium metal present in the product increases quite considerably upon switching from TiCl₄ to TiCl₃ in reactions with Li₃N. The α-Ti impurity in Figure 2b has larger lattice parameters (*a* = 2.972 Å, *c* = 4.792 Å) than titanium metal (*a* = 2.950 Å, *c* = 4.682 Å) which correlate to approximately 15–20 at% nitrogen dissolved in the metal lattice.³² Note also that the metallic impurity is still present when NaN₃ is used in place of Li₃N (Figure 2c) in a small scale reaction. Large scale reactions were performed using TiCl₃ with Li₃N and/or NaN₃. Figure 2d shows the presence of crystalline TiN again ac-

(29) (a) Steyermark, A. *Quantitative Organic Microanalysis*, 2nd ed.; Academic Press: New York, 1961. (b) Vogel, A. I. *Quantitative Inorganic Analysis*, 3rd ed.; John Wiley and Sons Inc.: New York, 1961.

(30) *CRC Handbook of Chemistry and Physics*, 66th ed.; Weast, R. C., Ed.; CRC Press, Inc.: Boca Raton, FL, 1985.

(31) *Binary Alloy Phase Diagrams*, 2nd ed.; Massalski, T. B., Ed.; ASM Intl.: Materials Park, OH, 1990.

(32) Wriedt, H. A.; Murray, J. L. *Bull. Alloy Phase Diag.* **1987**; 8(4), 378.

Table 1. X-ray Diffraction Results

Nitride ^a	lattice parameters		crystallite size (Å) ^b
	small [large] scale (<i>a</i> in Å) ^b	lit. for MN _{1.0} (<i>a</i> in Å)	
TiN	4.236(3) [4.2410(2)]	4.241(2) ³²	170 [490]
ZrN	4.5730(4) [4.5739(3)]	4.5730(5) ³⁹	210 [500]
HfN	4.5112(4)	4.515 ^{c,39}	180
NbN	4.3941(6) [4.3886(7)]	4.392 ^{42a}	390 [440]
TaN	4.3221(4)	4.329 ^{c,43a}	340
TaN(<i>P</i> ₆ ² m)	<i>a</i> = 5.1924(3)	<i>a</i> = 5.196(4)	570
hexagonal	<i>c</i> = 2.9081(3)	<i>c</i> = 2.911(2) ³⁹	

^a All products crystallize in the cubic NaCl structure (*Fm* $\bar{3}$ *m*) unless otherwise indicated. All reactions were with metal chlorides except TiN (small) where Ti₄ was used. The reactions have Li₃N:NaN₃ ratios of 1:0 except TiN (large), NbN (small), NbN (large), and TaN (small) which have 1:1.5, 1:10, 1:4.5, and 1:12 ratios, respectively. ^b Lattice parameters and crystallite sizes for large scale reaction products are in brackets. ^c Lattice parameter extrapolated to MN_{1.0} using data in reference.

accompanied by some α -Ti when Li₃N was the only nitriding agent. In an effort to decrease the amount of this nitrogen-deficient component, the nitrogen concentration in the reaction was increased by partially substituting Li₃N with NaN₃ (a more nitrogen-rich precursor). One mol of Li₃N was replaced by three mols of NaN₃ in order to maintain a salt-balanced equation. The molar ratio of lithium nitride to sodium azide used was 1:1.5. This resulted in a near elimination of the α -Ti phase (Figure 2e). Table 1 reports lattice parameters for the small and large scale products, makes comparisons to literature reports of stoichiometric (MN_{1.0}) nitrides, and lists crystallite sizes based on XRD line broadening.

Group 5 Nitrides. The synthesis of the group five nitrides resulted in two phase mixtures of crystalline nitrides when NbCl₅ or TaCl₅ were reacted with Li₃N alone. Both the cubic (NaCl-structure) mononitride phase and a nitrogen-deficient hexagonal (β -M₂N) phase were detected by X-ray diffraction. Note that there is a partial splitting of the XRD peaks in the cubic phase of NbN in Figure 3a. This probably results from cubic products with different nitrogen concentrations causing the lattice parameters to vary. As with the titanium case described above, the more nitrogen-rich precursor, NaN₃, was again partially substituted for Li₃N. As the ratio of Li₃N to NaN₃ was changed from 1:0 to 1:2 to 1:10, XRD results show a significant decrease in the M₂N phase and the enhancement of the mononitride product. This progression is shown for the case of the niobium nitride small scale reactions in Figure 3(a–c). A large scale reaction (20 mmol NbCl₅) successfully formed a single-phase cubic product (δ -NbN) using a Li₃N to NaN₃ ratio of 1:4.5 (Figure 3d).

A similar trend was seen in the tantalum system, where increasing the sodium azide to lithium nitride ratio favors the formation of the mononitride TaN. In this case, however, the mononitride is a mixture of the room-temperature hexagonal phase (ϵ -TaN) and a high-temperature cubic phase (δ -TaN) (Figure 3e). All the lattice parameters reported in Table 1 agree well with literature values for stoichiometric nitrides.

Magnetic Susceptibility. Previous studies have shown that there is a correlation between the transition temperature (*T*_c) and nitride composition of superconducting nitrides.³ Samples of ZrN and NbN from large scale reactions (Figures 1b and 3d) were analyzed for a superconducting transition. As Figure 4 shows, these compounds become superconducting at low temperatures. Their onset temperatures are 8.5 and 15.5 K for ZrN and NbN, respectively. These transitions correspond to approximate compositions of ZrN \sim 0.96 and NbN \sim 0.95 for the superconducting fraction in these samples. For comparison, a commercial ZrN sample exhibited a *T*_c of 7.5 K corresponding

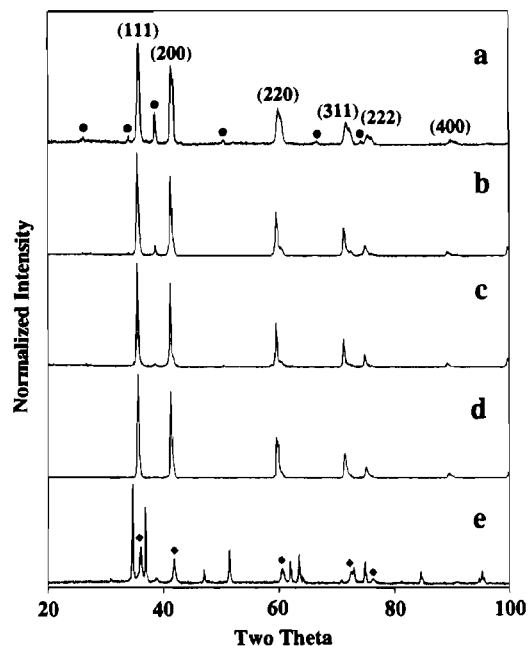


Figure 3. Powder XRD results of washed products from the reaction of 2 mmol NbCl₅ with Li₃N:NaN₃ in ratios of (a) 1:0; (b) 1:2; and (c) 1:10; and (d) 20 mmol NbCl₅ with Li₃N:NaN₃ (1:4.5). The cubic NbN peaks are labeled with their (*hkl*) values and the ● denotes β -Nb₂N. The products in (e) are from the reaction of 4 mmol TaCl₅ with Li₃N:NaN₃ (1:12). The δ -TaN (cubic) peaks are labeled by a ◆.

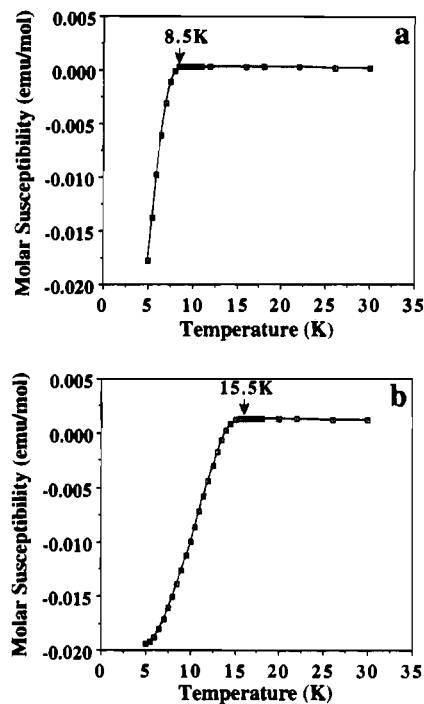


Figure 4. Magnetic susceptibility results from large scale, single-phase cubic nitrides of (a) ZrN from ZrCl₄ and Li₃N and (b) NbN from NbCl₅ and Li₃N:NaN₃ (1:4.5). The samples were cooled in a 2kG field prior to measurement.

to ZrN \sim 0.93. The magnitude of the molar susceptibility changes for the transitions are more than half that of the transition from a crystalline niobium powder standard. Note that the ZrN transition is not yet complete at 5 K so the above comparison is a lower limit in this case. The broad transition for NbN is indicative of a compound with some compositional inhomogeneity.³

Particle Size and Morphology. The XRD peaks are broad, indicating that these nitrides form as small crystallites. The average crystallite sizes determined from peak broadening are

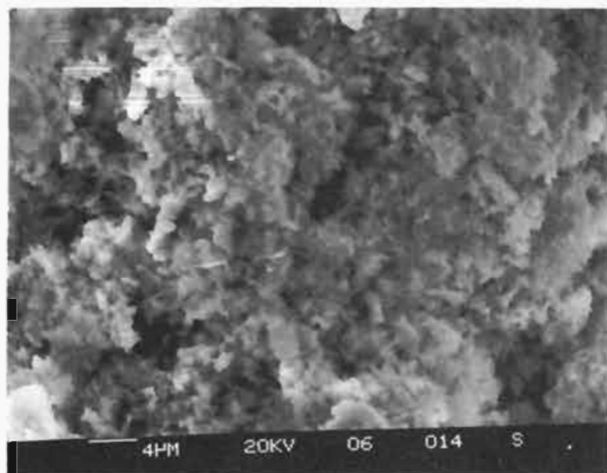


Figure 5. Scanning electron micrograph of the washed ZrN product resulting from the large scale reaction between $ZrCl_4$ and Li_3N .

nearly 200 Å for the small scale group four nitrides, while the large scale reaction products have sharper XRD peaks corresponding to crystallite sizes near 500 Å (see Figures 1 and 2 and Table 1). The NbN crystallite sizes are approximate due to some asymmetry in the XRD peaks. Scanning electron microscopy on the large scale ZrN washed product show it to be a fine powder with a morphology suggestive of agglomerations of hundreds of small crystallites resulting in particles with sizes ranging from about 0.1–10 μm (Figure 5). Previous reports on the ZrN reaction have shown that the unwashed products have a smooth, glassy morphology suggestive of a solidified melt, even at a 20 μm resolution using SEM. EDS indicated the presence of a considerable amount of chlorine consistent with a LiCl melt.¹⁴

In earlier studies on SSM reactions forming MoS_2 it was shown that the addition of an inert heat sink (e.g. NaCl) to the metathesis reaction results in products with lower crystallinity, as exemplified by significant broadening of the XRD lines.¹⁸ It is believed that the melting of the inert salt additive during the reaction removes heat normally available for crystallization of the product. The effect of an inert heat sink was investigated in the ZrN system where increasing amounts of NaCl were added to the reaction of $ZrCl_4$ (7 mmol) and Li_3N . The cubic nitride peaks generally broadened as more salt was added, indicating that the crystallite size was decreasing. Using $ZrCl_4$:NaCl molar ratios of 1:0, 1:1, 1:2, 1:3, 1:4 yielded products with relative crystallite sizes of 260 Å, 280 Å, 190 Å, 140 Å, and 140 Å, respectively. In addition, peaks for partially nitrated α -Zr became increasingly prominent as the amount of salt was increased. These salt additions are limited since beyond a 1:4 $ZrCl_4$:NaCl ratio the salt dilutes the precursors to such an extent that a self-propagating reaction is very difficult to initiate with a heated wire.

Analysis of Thermal Events. In order to better understand the propagation parameters in these reactions some important thermodynamic properties were measured with the zirconium nitride system serving as an example. Bomb calorimetry experiments gave a value of -165.0 kcal/mol (690.4 kJ/mol) for the heat of reaction between $ZrCl_4$ and Li_3N assuming 100% conversion. The reaction actually produced ZrN in a 91.6% yield based on product weights. After correcting for product yields, this results in a value of -180.1 kcal/mol (753.5 kJ/mol) for the heat released in the reaction forming ZrN and compares favorably to the ΔH_{rxn} of -191.6 kcal/mol (801.7 kJ/mol) calculated from Hess's law and standard thermodynamic values.^{33,34} Similar agreement has been observed previously in the MoS_2 system.¹⁸

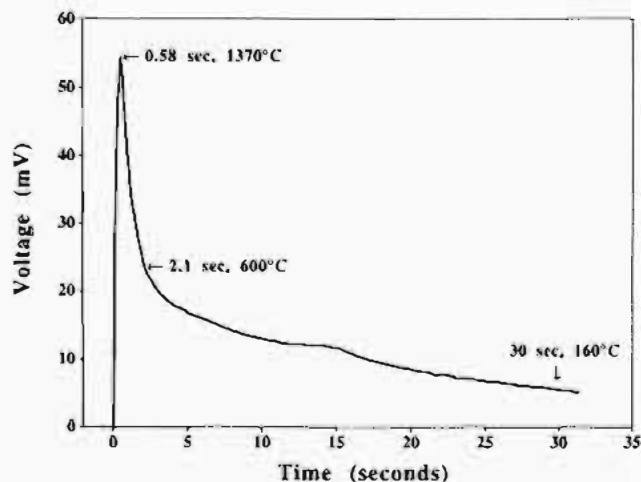


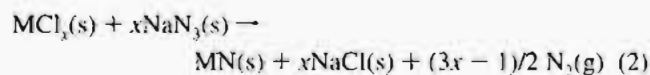
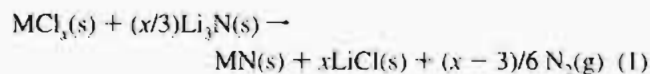
Figure 6. Measured reaction temperature profile using an *in situ* thermocouple for the reaction of 4 mmol $ZrCl_4$ with Li_3N . Time labels on the plot refer to time after reaction ignition.

An *in situ* thermocouple was used to measure the temperature profile in the ZrN reaction and a characteristic trace is shown in Figure 6. A sharp temperature rise follows the initiation of the powder precursor mixture by the hot filament. The peak reaction temperature of 1350–1400 °C is reached just 580 ms after initiation. The reaction cools rapidly to 600 °C within 2 s after initiation and approaches room temperature within 30 s. The speed of this cooling was found, not surprisingly, to depend on the amount of the reactants and the size of the reaction vessel. Note also that the response time of the thermocouple and chart recorder may contribute to the time required to reach the peak temperature making 580 ms a maximum value.

Precursor mixtures for ZrN ($ZrCl_4$ with either Li_3N or NaN_3) were heated in a DSC cell from room temperature to 600 °C (Figure 7). In both cases shown, there is a small but steady exothermic process beginning at about 150 °C and continuing until the reaction initiates. When the nitriding agent is Li_3N , the rapid exothermic reaction occurs at 440 °C (Figure 7a). This temperature increases by about 40 °C when the heating rate is slowed to 10 °C/min. With the less stable azide precursor, the rapid exothermic reaction occurs at 370 °C (Figure 7b).

Discussion

Initiation Process. The metathesis reaction schemes for solid metal chlorides (trihalides or greater) reacting with Li_3N or NaN_3 have the general form:



Previous reports suggest that these SSM reactions become self-propagating near temperatures where one of the precursor lattices begins to break down or undergoes a phase change (i.e. decomposition or sublimation).^{17,20} Since the metal halides used in this study sublime or decompose below 500 °C, the heated filament (~ 850 °C) is sufficiently hot to start a local exothermic

(33) (a) Kelly, K. K. *High Temperature Heat Content, Heat Capacity and Entropy Data for the Elements and Inorganic Compounds*. Bureau of Mines Bulletin 584; U.S. Government Printing Office: Washington D. C., 1960. (b) Barin, I.; Knacke, O. *Thermochemical Properties of Inorganic Substances*; Springer-Verlag: New York, 1973.

(34) *JANAF Thermochemical Tables*, 3rd ed.; Lide, D. R., Jr., Ed.; American Chemical Society and American Institute of Physics Inc.: New York, 1985.

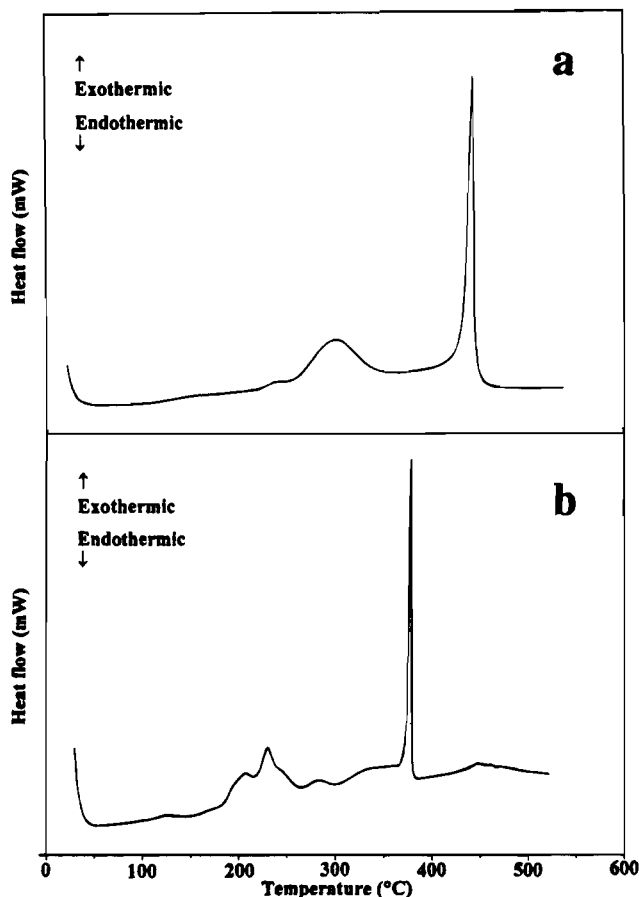


Figure 7. Differential scanning calorimetry results on sealed pans containing pellets of (a) ZrCl_4 and Li_3N and (b) ZrCl_4 and NaN_3 .

reaction which propagates quickly throughout the sample. The DSC results show that the initiation temperature in the ZrN system is higher when ZrCl_4 is reacted with Li_3N than when NaN_3 is used. The lower initiation temperature is expected in the azide case because NaN_3 exothermically decomposes to Na and N_2 by 365°C ,³⁵ while ZrCl_4 does not melt under pressure until temperatures near 410°C .³⁴ Li_3N is the most stable of the three reactants and does not melt until temperatures in excess of 800°C .³⁴ Roughly, the initiation temperatures correspond to the phase changes in the least stable precursor (370°C when NaN_3 is used and 440°C when Li_3N is used). Note that no endothermic events are evident, indicating that there is no significant ZrCl_4 sublimation prior to the start of the SSM reaction.

In both DSC plots there is a small broad exothermic event starting near 150°C and continuing to the initiation temperature. Since this event does not show up in the precursors alone, it suggests the occurrence of a small amount of surface reaction between the precursors. This phenomenon has been observed in other systems,²⁰ and has been utilized to make e.g. amorphous zirconium oxide¹⁶ by heating ZrCl_4 and Na_2O below their ignition point for several days.

Exothermic Propagation. The results from bomb calorimetry show that these reactions proceed quite well according to equation (1). Parkin et al.²⁵ have measured byproduct nitrogen gas pressures in some systems which also agree well with predictions. High speed photographs and optical pyrometry on the MoS_2 metathesis system have shown that reactions of this type can be very fast (< 1 s) and reach temperatures of at least

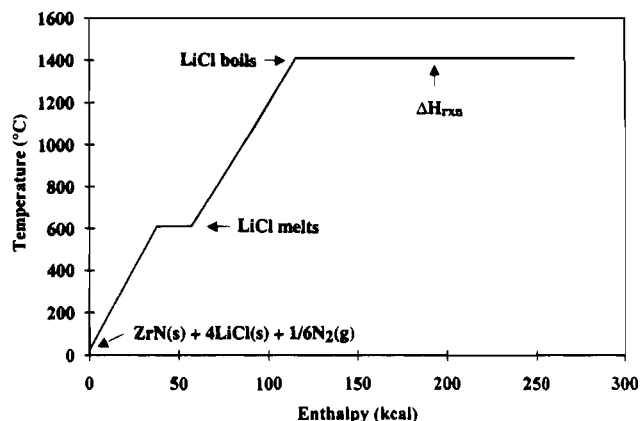


Figure 8. Theoretical enthalpy versus temperature plot for the reaction of ZrCl_4 and Li_3N .

1000°C .¹⁸ The *in situ* temperature measurements for ZrN show that these nitride SSM reactions also proceed very rapidly. The reaction speed allows one to consider these to be pseudo-adiabatic systems similar to other combustion reactions,¹² where essentially all of the heat released is used to raise the temperature of the products or cause phase changes. By applying the adiabatic assumption together with standard thermodynamic values including heat capacities and heats of transition for the reaction products,^{33,34} one can compute the steps on an enthalpy versus temperature curve.³⁶ Such a graph for the ZrN system ($\text{ZrCl}_4 + \text{Li}_3\text{N}$) is shown in Figure 8. As is common with metathesis systems of this type, the formation of many moles of salt causes the theoretical maximum temperature (i.e. the point where ΔH_{rxn} is exhausted) to equal the boiling point of the byproduct salt. Figure 8 shows that all of the available enthalpy is used up when nearly half of the LiCl is vaporized (bp 1408°C). Evidence for salt vaporization comes from its presence on the lid of the reaction bomb and previous reports of salt vaporization during sealed tube metathesis reactions.^{25b} Figure 6 shows experimental results which validate these theoretical predictions since maximum temperatures near 1400°C are measured by the *in situ* thermocouple.

Chemical Reactions. Lithium nitride is a good choice as a solid nitrogen precursor source due to its thermal stability which allows it to deliver nitrogen in high temperature environments. It also has a reducing nature (N^{3-}) and is very reactive. Since most of the metal halides studied here contain highly oxidized metals (+4, +5), they must be reduced to at least M^{3+} to form the nitride, resulting in a net redox process. Two possible mechanisms for these metathesis reactions involve: (a) initial formation of the byproduct salt with a reduction of the metal and oxidation of the nitrogen source(s) to their elemental states, followed by a reaction of finely divided metal and nitrogen gas in a molten salt flux; or (b) simultaneous metal nitride and salt formation from an ionic flux containing molten salt and dissolved precursors. Previously studied systems exhibit characteristics pointing to primarily different pathways.^{19a,20b,21b}

While it is difficult to prove an ionic reaction pathway, the presence of unreacted metal in incomplete or quenched reactions may indicate elemental intermediates. The TiN system shows that when an easily decomposed metal halide is used (TiCl_3), the amount of subnitrided metal is significantly greater than when a sublimable halide (TiI_4) is used. TiCl_3 is known to disproportionate to $\text{TiCl}_4 + \text{TiCl}_2$ above 500°C and TiCl_2 then decomposes to Ti and TiCl_4 when heated further.³⁷ This information coupled with the XRD results suggests that the

(35) Richter, T. A. In *Energetic Materials 1: Physics and Chemistry of Inorganic Azides*; Fair, H. D., Walker, R. F., Eds.; Plenum Press: New York, 1977, p 33.

(36) TMAX Fortran program by R. M. Jacobinas, Department of Chemistry, University of California, Los Angeles.

decomposition of TiCl_3 precedes nitride formation, but with TiI_4 , these two processes may occur simultaneously. Full conversion to TiN using TiCl_3 then requires a large excess nitrogen concentration which can be produced by NaN_3 decomposition. In the niobium and tantalum systems, thermodynamically stable substoichiometric M_2N phases formed when Li_3N was used alone, yet again pure mononitride phases could be formed when large excesses of nitrogen were generated by using sodium azide.

The actions of the salt flux and thermodynamics also have an effect on the nature of the reaction products. In the study in which NaCl was added to the reaction mixture of ZrCl_4 and Li_3N , the presence of partially nitrated metal increased as the amount of the salt flux increased. All of the above observations suggest at least a partial elemental route since each reaction has enough nitrogen to produce stoichiometric mononitrides but various factors including decomposition of precursors, dilution in a salt flux, and thermodynamically stable subnitrides often prevent nitrogen from fully reacting with the metal.

Product Crystallization. After the SSM reaction between the precursors occurs, a high-temperature but short lived molten salt flux is generated. As Figure 6 shows, this LiCl salt flux is molten for only a few seconds before the temperature drops below its melting point (610°C). It is probable that the salt flux aids in the crystallization of these refractory nitrides as it often does in traditional crystal growth.³⁸ The products of large scale reactions are clearly more crystalline than their small scale counterparts (see Table 1), likely due to a larger and more efficiently insulated reaction core, allowing for increased product crystallization in the molten salt flux.

In addition to serving as a crystallization medium, the salt byproduct (LiCl , NaCl , etc.) also acts as a heat sink in the reaction. Since the process of melting requires large amounts of enthalpy, this limits the maximum reaction temperature (see Figure 8). When excess salt is added to the ZrN precursor mixture its presence causes the nitride product to become less crystalline. The salt removes heat from the system that would otherwise have been used for heating and product crystallization. The nitride crystallite size is reduced significantly through the addition of excess salt.

Nitrogen Precursor Effects. The nitrogen concentrations in these transition-metal nitride systems can clearly exhibit wide variation.^{1,39} The metals accept from a few atomic percent to nearly 20 at% nitrogen before other phases appear.^{32,40} There are also thermodynamically stable subnitrides M_2N (e.g. when $\text{M} = \text{Nb}$ or Ta) and the cubic mononitrides can exist substoichiometrically ($\text{N}/\text{M} < 1$) and occasionally hyperstoichiometrically ($\text{N}/\text{M} > 1$).¹ These compositional changes manifest themselves through changes in lattice parameters and physical properties. For instance, for both TiN and NbN the cubic lattice parameter increases up to $\text{MN}_{1.0}$ and decreases for $\text{N}/\text{M} > 1$.¹ In some of these rapid SSM reactions the Li_3N precursor alone is adequate to produce solely mononitride products. In cases where metal or substoichiometric phases are produced it is necessary to run these reactions in a very nitrogen-rich environment in order to obtain the mononitride. Increasing the excess nitrogen concentration or pressure in these reactions is achievable by partially substituting the alkali metal rich nitrating agent,

Li_3N , with a more nitrogen-rich one, NaN_3 . An examination of equations (1) and (2) shows that the main differences encountered in replacing Li_3N by NaN_3 is the production of a larger amount of nitrogen gas. For example, the reaction of NbCl_5 with Li_3N generates only 0.33 mol of N_2 , but 7 mols of N_2 can be produced when NaN_3 is used. If the ideal gas law is applied to the small scale niobium nitride study (assuming $T = 300\text{ K}$), the nitrogen gas pressure in the reaction vessel increases from 0.4 atm to 3.3 atm to 7 atm as the Li_3N to NaN_3 ratio increases from 1:0 to 1:2 to 1:10, respectively. The same holds true for the large scale (TiCl_3) titanium nitride case where the N_2 pressure increases from zero to 15 atm as the Li_3N to NaN_3 ratio changes from 1:0 to 1:1.5. In both the TiN and NbN cases, the increased nitrogen pressure correlates with a dramatic decrease in the amount of partially nitrated material in the product. The importance of reaction size as it relates to pressure is seen in the niobium nitride system where the large scale reaction with only a 1:4.5 Li_3N to NaN_3 ratio has a corresponding nitrogen pressure of 47 atm and results in a single phase product. These pressures represent lower limits since they would be nearly six times higher if calculated at the maximum reaction temperature.

The homogeneity of the cubic products is also effected by the reaction scale and nitrogen pressures. The small scale reactions of TiN and NbN (Figures 2a and 3c) have X-ray diffraction peaks which are slightly asymmetric and tail off at higher 2θ angles. This suggests the existence of a small amount of material with a slightly smaller lattice parameter corresponding to a cubic phase with a lower nitrogen concentration than the bulk product. Note, however, that the TiN XRD peaks of the large scale product made from the lithium nitride-sodium azide mixture are quite symmetric, indicating a more homogeneously nitrated product. In the NbN system, the tailing decreases as the reaction scale and azide substitution increases, although a slight asymmetry remains even in the large scale product. This asymmetry is mirrored in the broadness of its superconducting transition (Figure 4b), suggesting that some compositional variation still exists.³

Since NbN and TaN have cubic and hexagonal stoichiometric forms, it is of interest to consider how pressure and temperature determine which phase is produced. The hexagonal (ϵ) phase is readily produced by heating the metals in 1 atm N_2 at 1000°C .⁴¹ The cubic (δ) phases are more difficult to synthesize and require high nitrogen pressures (20 to 160 atm) and higher temperatures ($>1200^\circ\text{C}$ for NbN ,⁴² $>1600^\circ\text{C}$ for TaN ⁴³). It is therefore surprising that these metastable cubic phases are produced in these metathesis reactions since the maximum possible pressures are generally below the required range and the high temperatures are sustained for only seconds. It may be that these phases are more accessible because this metathesis scheme pairs up very reactive precursors containing isolated metal and nitrogen species. If, as the results suggest, these reactions proceed via elemental intermediates, the very small particles of metal which are produced in the molten salt flux may be very reactive towards nitrogen and these high temperature/high pressure phases are quenched rapidly in the melt. The presence of a mixed-phase product in the TaN reaction can be understood since the transition from ϵ - TaN to δ - TaN (~ 1600 – 1700°C)^{43a} is actually above the maximum reaction

(37) (a) Schumb, W. C.; Sundström, R. F. *J. Am. Chem. Soc.* **1933**, *55*, 596. (b) Farber, M.; Darnell, A. J. *J. Chem. Phys.* **1956**, *25*(3), 526 and 531.

(38) Scheel, H. J.; Elwell, D. *Crystal Growth from High Temperature Solutions*; Academic Press: New York, 1975.

(39) *Pearson's Handbook of Crystallographic Data for Intermetallic Phases*, 2nd ed.; Villars, P.; Calvert, L. D. Eds.; ASM Intl.: Materials Park, OH, 1991.

(40) (a) Domagala, R. F.; McPherson, D. J.; Hansen, M. *J. Met. Trans. AIME* **1956**, *8*, 98. (b) Taylor, A.; Doyle, N. J. *J. Less-Common. Met.* **1967**, *13*, 413.

(41) (a) Guard, R. W.; Savage, J. W.; Swarthout, D. G. *Trans. Metall. AIME* **1967**, *239*, 643. (b) Schönberg, N. *Acta Chem. Scand.* **1954**, *8*(2), 199.

(42) (a) Brauer, G.; Kirner, H. Z. *Anorg. Allg. Chem.* **1964**, *328*, 34. (b) Lengauer, W.; Etmayer, P. *Monat. Chem.* **1986**, *117*, 275.

(43) (a) Gatterer, J.; Dufek, G.; Etmayer, P.; Kieffer, R. *Monat. Chem.* **1975**, *106*, 1137. (b) Kieffer, R.; Etmayer, P.; Freudhofmeier, M.; Gatterer, J. *Monatsh. Chem.* **1971**, *102*, 483.

temperature obtainable in this reaction (1408 °C). Recent studies have shown that ϵ -TaN can be converted to δ -TaN by subjecting the material to a very rapid shock wave equivalent to 120,000 atm.⁴⁴ Since these rapid SSM nitride reactions are generally violent in nature, there may also be a shock wave component aiding in the formation of the observed phases. Efforts are continuing in an attempt to isolate single-phase δ -TaN through variations in precursors and reaction conditions.

Conclusions

Transition-metal nitrides of titanium, zirconium, hafnium, niobium, and tantalum are formed from rapid solid-state metathesis (SSM) reactions of metal halides with Li_3N . These self-propagating reactions initiate at temperatures near a phase change or decomposition point of one of the precursors and reach high temperatures (near 1400 °C) very quickly. The presence of elements and M_2N phases in some products is suggestive of elemental intermediates in these reactions. The product crystallite sizes increase with the size of the reaction

likely due to a more efficient use of the heat generated in the reaction which maintains the byproduct salt in a molten state for a longer period. In most cases these nitrides form cubic, rock-salt structures, though sometimes it is necessary to partially substitute lithium nitride with sodium azide to generate the high nitrogen pressures necessary to produce single-phase products. With sufficient substitution, the high internally generated nitrogen gas pressures allow the formation of phases such as δ -NbN and δ -TaN which are normally only synthesized at high temperatures and pressures.

Acknowledgment. The authors thank Prof. John Wiley for helpful discussions and critical review of this manuscript, Dr. Rande Treece for insight into reaction mechanisms and invaluable assistance with the magnetic susceptibility measurements, Dr. Dave Winter for help with the ICP-AA measurements, and Ms. Janice Allen (NSF Summer Research Program in Solid State Chemistry) for performing the study on salt addition in the ZrN system. This work was supported by the National Science Foundation Grant DMR-9315914 and the Packard, Dreyfus, and Sloan Foundations (R.B.K.).

(44) Mashimo, T.; Tashiro, S.; Toya, T.; Nishida, M.; Yamazaki, H.; Yamaya, S.; Oh-ishi, K.; Syono, Y. *J. Mater. Sci.* **1993**, *28*, 3439.